



Article

Shape Memory Effect and Superelasticity of [001]-Oriented FeNiCoAlNb Single Crystals Aged under and without Stress

Yuriy I. Chumlyakov ¹, Irina V. Kireeva ^{1,*}, Zinaida V. Pobedennaya ¹, Philipp Krooß ²  and Thomas Niendorf ² 

¹ Siberian Physical Technical Institute, National Research Tomsk State University, 634050 Tomsk, Russia; chum@phys.tsu.ru (Y.I.C.); pobedennaya_zina@mail.ru (Z.V.P.)

² Institute für Werkstofftechnik, Universität Kassel, 34125 Kassel, Germany; krooss@uni-kassel.de (P.K.); niendorf@uni-kassel.de (T.N.)

* Correspondence: kireeva@spti.tsu.ru or v.kireeva@mail.ru; Tel.: +7-960-972-1175

Abstract: The two-step ageing of Fe-28Ni-17Co-11.5Al-2.5Nb (at.%) single crystals under and without stress, leads to the precipitation of the γ' - and β -phase particles. Research has shown that γ - α' thermoelastic martensitic transformation (MT), with shape memory effect (SME) and superelasticity (SE), develops in the [001]-oriented crystals under tension. SE was observed within the range from the temperature of the start of MT upon cooling M_s , to the temperature of the end of the reverse MT upon heating A_f , and at temperatures from A_f to 323–373 K. It was found that at γ - α' MT in the [001]-oriented crystals, with γ' - and β -phase particles, a high level of elastic energy, ΔG_{el} , is generated, which significantly exceeds the energy dissipation, ΔG_{dis} . As a result, the temperature of the start of the reverse MT, while heating A_s , became lower than the temperature M_s . The development of γ - α' MT under stress occurs with high values of the transformation hardening coefficient, $\Theta = d\sigma/d\varepsilon$ from 2 to 8 GPa and low values of mechanical $\Delta\sigma$ and thermal ΔT_h hysteresis. The reasons for an increase in ΔG_{el} during the development of γ - α' MT under stress are discussed.

Keywords: iron-based shape memory alloy; single crystals; particles of γ' - and β -phase; superelasticity; tension



Citation: Chumlyakov, Y.I.; Kireeva, I.V.; Pobedennaya, Z.V.; Krooß, P.; Niendorf, T. Shape Memory Effect and Superelasticity of [001]-Oriented FeNiCoAlNb Single Crystals Aged under and without Stress. *Metals* **2021**, *11*, 943. <https://doi.org/10.3390/met11060943>

Academic Editor: Joan-Josep Suñol

Received: 14 May 2021

Accepted: 7 June 2021

Published: 10 June 2021

Publisher's Note: MDPI stays neutral with regard to jurisdictional claims in published maps and institutional affiliations.



Copyright: © 2021 by the authors. Licensee MDPI, Basel, Switzerland. This article is an open access article distributed under the terms and conditions of the Creative Commons Attribution (CC BY) license (<https://creativecommons.org/licenses/by/4.0/>).

1. Introduction

FeNiCoAlX alloys (X = Ta, Nb, Ti), undergoing thermoelastic martensitic transformation (MT) from the fcc (γ)-phase to bct (α')-martensite upon cooling/heating and under stress, are characterized by high values of superelasticity (SE) from 5 to 13.5% and values of shape memory effect (SME) of up to 8%; these alloys can compete with TiNi-based alloys [1–34]. The necessary conditions for the development of thermoelastic γ - α' MT are achieved: (i) due to the precipitation of nanosized γ' -phase particles, with $L1_2$ -type ordering of between 3 and 8 nm in size, which have coherent lattice conjugation with high-temperature γ -phase and retain coherence during MT in α' -martensite [1–4,28]; (ii) particles of the γ' -phase strengthen the high-temperature phase, reduce the transformation strain by comparison with the single-phase state [1,5] and contribute to an increase in the tetragonality of martensite c/a to 1.1–1.23 [1,28]. This, in turn, decreases the value of the shear strain, g , at γ - α' MT and the Burgers vector, b , of twinning dislocations $a/6\langle 211 \rangle(111)$, arising during MT [1–5,18].

In the FeNiCoAlX polycrystals (X = Ta, Nb, Ti) during ageing at high temperatures, $T \sim 873$ – 973 K, the precipitation of β -phase particles with B2-type ordering at the grain boundaries occurs simultaneously with the precipitation of γ' -phase particles in the grain body, leading to a catastrophic decrease in plasticity [5,31,32]. Alloying with boron to 0.05 at.% suppresses the precipitation of β -phase particles along the grain boundaries, which contributes to the manifestation of SME and SE in the polycrystals of these alloys [5,31,32]. In addition, an increase in the grain size to 100–200 μm and the creation of a sharp $\langle 001 \rangle\{035\}$ texture in polycrystals, as well as the production of oligocrystals, leads to the appearance of SE from 5 to 13.5% in these alloys [5,6,31,32].

Studies of γ - α' MT on the FeNiCoAlX single crystals ($X = \text{Ta, Nb, Ti}$) have a number of advantages over polycrystals. Firstly, single crystals make it possible to study the orientation dependence and asymmetry under the tension and compression of SME and SE [11–15,17,27]. These results are necessary for the development of micromechanical models in the development of a γ - α' MT under stress in polycrystals with different textures. Secondly, earlier studies of the FeNiCoAlX single crystals ($X = \text{Ta, Nb, Ti}$) showed that the precipitation of β -phase particles in single crystals, in contrast with the polycrystals, does not lead to a loss of plasticity [5,25,31–34]. Thirdly, nanosized β -phase particles, which are precipitated in single crystals at 973 K, with an ageing time of $t \geq 7$ h, in relation to one- and two-step ageing, lead to an increase in MT temperatures, the retention of SME and SE from 3 to 8%, the appearance of rubber like elasticity and the development of SE in the temperature range from M_s to A_f [13,19,33,34].

In the present paper, on the Fe-28Ni-17Co-11.5Al-2.5Nb (FeNiCoAlNb) (at.%) single crystals oriented along the [001] direction, the task was to investigate the temperature dependence of the stresses, $\sigma_{cr}(T)$, required for the onset of stress-induced γ - α' MT, SE and its temperature range, SME and the value of thermal ΔT_h and mechanical $\Delta\sigma$ hysteresis, using ageing methods under and without stress under tension. The choice of ageing under and without stress is due to the following. In alloys with coherent non-equiaxial particles, ageing under stress leads to the predominant growth of one variant of particles and the appearance of the internal oriented stresses, which are absent during ageing without stress [35–37]. In the case of precipitation of non-coherent and non-equiaxed particles after ageing without stress, internal stresses do not arise due to the formation of dislocations at the “particle-matrix” boundaries [29,30]. The effect of ageing under stress on the precipitation of non-coherent β -phase particles in the FeNiCoAlX alloys ($X = \text{Ta, Nb, Ti}$) has not yet been studied. In the present paper, such experiments using FeNiCoAlNb single crystals oriented along the [001] direction are presented for the first time.

2. Materials and Methods

Ingots of the Fe-28Ni-17Co-11.5Al-2.5Nb (FeNiCoAlNb) (at.%) alloy were melted from pure elements in a resistance furnace (InterSELT, St. Petersburg, Russia) in a helium atmosphere. To achieve a homogeneous distribution of the elements in the bulk of the ingots, they were remelted three times. Single crystals of the FeNiCoAlNb alloy were grown by the Bridgman method in a helium atmosphere, on a Russian-made Redmet installation (Firm “Kristaloptika”, Tomsk, Russia). To determine the orientation of the crystals, the diffractometric method was used by means of a DRON-3M X-ray diffractometer (Bourestnik, St. Petersburg, Russia) with monochromatic Fe $K\alpha$ radiation. Dog-bone-shaped tension samples had a gauge length of 12 mm and a cross section of $2 \times 1.5 \text{ mm}^2$. Samples were cut using wire electrical discharge machining ARTA-5.9 (DELTA-TEST, Fryazino, Moscow region, Russia). The damaged surface layer was ground off mechanically, and then electrically polished in 200 mL of an $\text{H}_3\text{PO}_4 + 50 \text{ g CrO}_3$ (phosphoric acid with chromium trioxide) electrolyte at room temperature. All samples were initially homogenized at 1573 K for 24 h in a quartz tube, in a helium atmosphere, followed by water quenching. Two-step ageing was used to precipitate γ' - and β -phase particles. The first step of ageing was carried out at a temperature of 973 K for 5 h without stress, in an MRU-STF15180-01_301 resistance furnace (Carbolite Gero, Hope Valley, UK) within a quartz tube, in a helium atmosphere with water quenching. The second step of ageing was performed in a vacuum at 873 K, for 2 and 4 h in a special device (Firm “Kristaloptika”, Tomsk, Russia) with a vacuum chamber, able to apply tensile stresses of 120 MPa during ageing, in the following way. Two samples were simultaneously used during each ageing treatment in the second step, with their axes in vertical and horizontal positions. The temperature was monitored by a thermocouple, attached to the vertical sample. The device was pre-heated to 473 K, subsequently, a constant tensile stress of 120 MPa was applied to the vertical sample, whereas the horizontal sample remained in a stress-free condition. Next, the device was heated to 873 K at a rate of 20 K/min and kept for 2 h and 4 h at 873 K. A controlled stress

of 120 MPa, applied to the vertical sample, was maintained during all the ageing treatment. The simultaneous ageing of two samples (under and without applied stress) allows for a better comparison of these, to ascertain the effect of the applied external stress, as the samples adhere to exactly the same temperature evolutions during ageing. After completion of the ageing process under stress, the device was slowly cooled to 373 K over 1.5 h and unloaded. Start M_s and finish M_f temperatures of the forward γ - α' MT during cooling and start A_s and finish A_f temperatures of the reverse γ - α' MT during heating, were determined by the intersection of tangents on the temperature dependence of the electrical resistance $\rho(T)$ on a Russian-manufactured installation (Firm "Kristalloomoptika", Tomsk, Russia). The MT temperatures under stress were determined in terms of deviation from the linear dependence in the "transformation strain-temperature" ($\varepsilon_{tr}(T)$) curves. The value of thermal ΔT_h and mechanical $\Delta\sigma$ hysteresis was determined in the middle of the $\varepsilon_{tr}(T)$ and "stress-strain" ($\sigma(\varepsilon)$) hysteresis loops, respectively. Mechanical properties and SE were investigated using an Instron 5969 universal testing machine (Instron, Norwood, MA, USA) at the deformation rate of $4 \cdot 10^{-4} \text{ s}^{-1}$. Tests at room temperature were carried out in air. Tests within the temperature range of 185–350 K were carried out in a special cooling/heating chamber, which is included in the equipment of the Instron 5969 universal testing machine (Instron, Norwood, MA, USA). The heating/cooling rate of the chamber was 2 K/min. The sample was inserted into grips, heated/cooled together with the chamber, kept at each temperature for 30 min before testing, and then deformed. SME at a constant tensile stress in the cycle, was studied using a Russian-made dilatometer (Firm "Kristalloomoptika", Tomsk, Russia) during cooling and heating within a temperature range of 77–400 K, with a heating/cooling rate of 10 K/min. Temperature variations at $\sim 10 \text{ K/min}$ were achieved by liquid nitrogen, flowing in copper tubes, coiled around the grips and by induction heating of the grips. The sample temperature was measured by a thermocouple, fixed to the sample gauge section. The lowest sample temperature, attainable by the dilatometer, was $\sim 77 \text{ K}$. A miniature extensometer, attached to the sample, was used for the strain measurements. The crystal structure after ageing was investigated using a JEOL-2010 transmission electron microscope (TEM) (JEOL, Tokyo, Japan) at an accelerating voltage of 200 kV. The thin foils were prepared using double-jet electropolishing (TenuPol-5, "Struers", Ballerup, Denmark), with an electrolyte containing 20% sulfuric acid in methyl alcohol at room temperature, with 12.5 V applied voltage. In this paper, the following denotations are adopted for heat treatments: Crystal I—ageing without stress at 973 K for 5 h and then at 873 K for 2 h without stress and with slow cooling; Crystal II—ageing without stress at 973 K for 5 h and then ageing under stress 120 MPa at 873 K for 2 h with slow cooling; Crystal III—ageing at 973 K for 5 h, then at 873 K for 4 h without stress and with slow cooling; and Crystal IV—ageing without stress at 973 K for 5 h and then ageing under stress 120 MPa at 873 K for 4 h with slow cooling. For each ageing type, namely, Crystals I–IV, SE and SME were investigated on separate samples after determining the MT temperatures.

3. Results and Discussion

3.1. Effect of Ageing under and without Stress on Temperatures of γ - α' MT and the Precipitation of γ' - and β -Phase Particles

The temperatures of γ - α' MT, depending on the ageing condition under and without stress, and determined from the temperature dependence of the electrical resistivity $\rho(T)$, are presented in Figure 1 and Table 1. It may be observed that in Crystals III with regard to two-step ageing, an increase in the ageing time at the second step at 873 K from 2 to 4 h without stress leads to an increase in the M_s temperature by 29 K compared to Crystals I. In Crystals II and IV, ageing under stress at the second step leads to an increase in the M_s temperature by 15 and 11 K, respectively, relative to Crystals I and III.

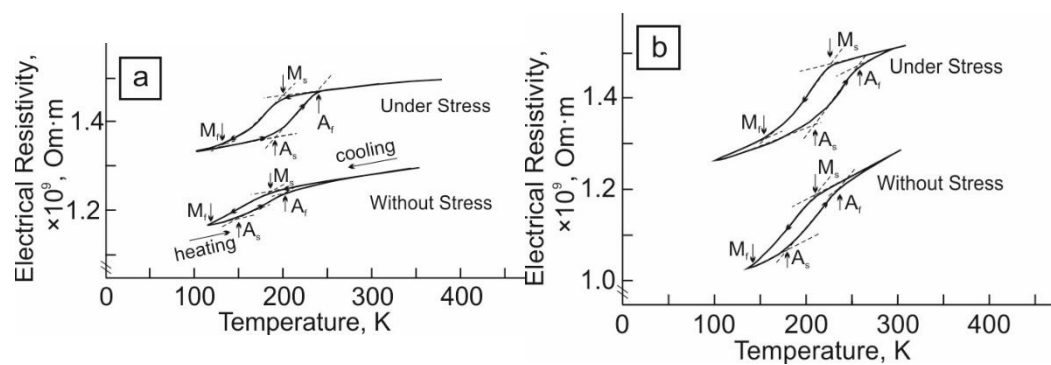


Figure 1. Temperature dependence of electrical resistivity $\rho(T)$ in the FeNiCoAlNb single crystals after two-step ageing: (a) ageing at 873 K for 2 h at the second step; (b) ageing at 873 K for 4 h at the second step.

Table 1. Characteristics of γ - α' MT in the FeNiCoAlNb single crystals after ageing under and without stress, obtained from the analysis of the temperature dependence of the electrical resistivity $\rho(T)$: $\Delta T_h = A_f - M_s$ is the thermal hysteresis; $\Delta M = M_s - M_f$ is overcooling; $\Delta A = A_f - A_s$ is overheating; ΔG_{el} is the stored elastic energy; ΔG_{dis} is the dissipated energy.

Crystals	M_s , K	M_f , K	A_s , K	A_f , K	ΔT_h , K	ΔM , K	ΔA , K	$\Delta G_{el}/\Delta G_{dis}$
Crystal I	185	120	150	203	18	65	53	6.6
Crystal II	200	130	190	240	40	70	50	3
Crystal III	214	140	180	235	21	74	55	6.5
Crystal IV	225	155	210	260	35	70	50	3.7

TEM studies (Figure 2) showed that in Crystals I–IV, the γ' - and β -phase particles are precipitated. The γ' -phase particles of the equiaxed shape, with $L1_2$ -type ordering, which is confirmed by the presence of superstructural reflections (Figure 2c), have the chemical composition, $(FeNiCo)_3AlNb$ [5,13,19,31,32]. Equiaxial γ' -phase particles have a size $d \sim 8$ –12 nm and coherent conjugation with the high-temperature γ -phase. These data are consistent with previously published results in [5,13,19,31,32]. TEM studies have shown that the particle size of the γ' -phase depends weakly on the ageing time at the second step and the external, applied stresses during ageing (Figure 2a,b).

The β -phase particles of the non-equiaxial shape with B2-type ordering have the chemical composition, $(FeNiCo)(AlNb)$ [31,32] and are non-coherent with the high-temperature γ -phase (Figure 2d,e). Due to the significant difference in the lattice parameters ($a_\gamma = 0.36$ nm, $a_\beta = 0.28$ nm), the β -phase particles lose coherence at small sizes, $d < 5$ nm [35]. Similar lattice parameters of the γ - and β -phases were obtained in the FeNiCoAlTaB polycrystals ($a_\gamma = 0.3604$ nm, $a_\beta = 0.2880$ nm) [5,31,32]. In the FeNiCoAlTaB polycrystals, β -phase particles are precipitated at the grain boundaries with the formation of regions free from γ' -phase particles. In these polycrystals, the nucleation of β -phase particles was also found on the Ta particles, with a lattice parameter close to the β -phase. The Ta particles decrease the energy barrier, associated mainly with the generation of elastic energy, for the β -phase nucleation [31,38]. In the FeNiCoAlNb single crystals, β -phase particles are precipitated in the volume of the crystal, and zones free from γ' -phase particles are not observed. During ageing without and under stress at the second step, four crystallographically equivalent variants of the β -phase particles, with an orientation relationship $(111)_\gamma \parallel (110)_\beta$, $[1\bar{1}0]_\gamma \parallel [1\bar{1}1]_\beta$, are formed (Figure 2d–f) [29,38]. With an increase in the ageing time at the second step, the volume fraction and particle size of the β -phase increase from $f = 0.1$, $d = 10$ –15 nm and $l = 35$ –40 nm at 2 h, to $f = 0.15$, $d = 22$ –35 nm and $l = 100$ –135 nm at 4 h (Figure 2d,e). Ageing under a tensile stress of 120 MPa does not lead to a notable difference in the morphology of the particles of the γ' - and β -phases compared to ageing without stress. In crystals aged under stress, an increased dislocation density was observed

at the “matrix- β -phase” interface (Figure 2e), which was less pronounced during ageing without stress.

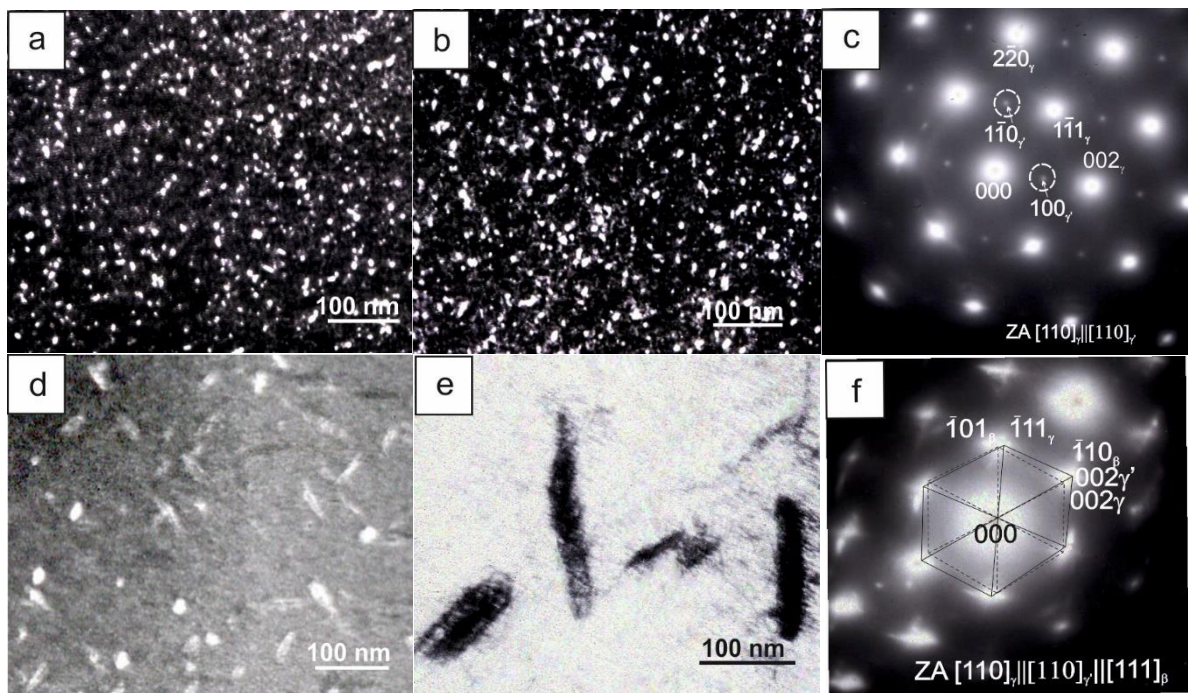


Figure 2. Transmission electron microscope (TEM) investigation of structure of the [001]-oriented FeNiCoAlNb crystals after two-step ageing: (a) dark-field image of γ' -phase particles in the γ' -phase reflex after ageing at 873 K for 2 h without stress at the second step; (b) dark-field image of γ' -phase particles in the γ' -phase reflex after ageing at 873 K for 4 h under stress at the second step; (c) diffraction pattern showing reflections of γ' -phase particles that are observed in case (a,b); (d) bright-field image of β -phase particles after ageing at 873 K for 2 h at the second step without stress; (e) bright-field image of β -phase particles after ageing at 873 K for 4 h at the second step under stress of 120 MPa; (f) corresponding diffraction pattern to (b,c).

TEM studies facilitate an explanation of the dependence of the M_s temperature on the ageing conditions [2]. Firstly, in Crystals I–IV, the volume fraction and particle size of the γ' -phase change insignificantly (Figure 2a,b) and, therefore, the M_s temperature change is not associated with this phase. Secondly, in Crystals I–IV, the volume fraction and particle size of the β -phase change in relation to the ageing time at the second step. The volume fraction and size of β -phase particles are larger in Crystals III and IV, than in Crystals I and II. This leads to a decrease in the nickel concentration in the matrix and explains the increase in the M_s temperature in Crystals III and IV, in comparison with Crystals I and II [1–6,38]. Thirdly, the differences in the sizes and volume fractions of β -phase particles, as a consequence of the ageing conditions under and without stress, were not found in the study of the crystal structure. Consequently, an increase in the M_s temperature in Crystals II and IV compared to Crystals I and III, respectively, cannot be explained from the standpoint of changes in the concentration of alloying elements in the matrix, and in the morphology of the particles of the γ' - and β -phases. The increase in the M_s temperature in Crystals II and IV in comparison with Crystals I and III is due to the formation of internal oriented stress fields $\langle\sigma_G\rangle$ from the β -phase particles. A qualitative confirmation of the $\langle\sigma_G\rangle$ appearance is the formation of dislocations at the “matrix- β -phase” boundaries (Figure 2e), as was previously observed in TiNi crystals, aged under stress and containing partially non-coherent Ti_3Ni_4 precipitates [29,30,39,40].

As can be seen in Table 1, γ - α' MT during heating-cooling in a free state, is associated with thermoelastic MT of the second type, in which $A_s \leq M_s$ [29,30,41]. Another feature is the large value of overcooling $\Delta M = M_s - M_f$, with a forward γ - α' MT and overheating of $\Delta A = A_f - A_s$ with a reverse α' - γ MT, varying from 50 to 74 K in combination with

low values of thermal hysteresis, $\Delta T_h = A_f - M_s = 18\text{--}40$ K. According to the results of thermodynamic analysis for the thermoelastic MT of the second type [41–45], the ratio of the stored elastic energy, ΔG_{el} , is equal to or exceeds the doubled value of the dissipated energy, $2\Delta G_{dis}$, $\Delta G_{el} \geq 2\Delta G_{dis}$. The values of ΔG_{el} and ΔG_{dis} are estimated from the relationships obtained in [33,41–45]:

$$\Delta G_{el} = \frac{\Delta S_{ch}}{2}(M_s - M_f) + \frac{\Delta S_{ch}}{2}(A_f - A_s) \quad (1)$$

$$\Delta G_{dis} = \frac{\Delta S_{ch}}{2}(A_f - M_s) \quad (2)$$

M_s , M_f and A_s , A_f are, respectively, the temperatures of the start and finish of the forward $\gamma\text{--}\alpha'$ MT during cooling and the reverse during the heating of the $\alpha'\text{--}\gamma$ MT; ΔS_{ch} is the change in entropy under MT. Estimates show that $\Delta G_{el}/\Delta G_{dis}$ varies from 3 to 6.6 (Table 1). High values of ΔG_{el} , as will be shown below, determine the temperature range of SE in Crystals I–IV.

3.2. SE and SME in the [001]-Oriented FeNiCoAlNb Crystals Aged under and without Stress

SE in Crystals I–IV was found within a broad temperature range (Figure 3). A comparison of the $\gamma\text{--}\alpha'$ MT temperatures, obtained from the $\rho(T)$ dependence (Figure 1) and the SE temperature range (Figure 3), shows that SE in Crystals I–IV takes place at M_s temperature, within the temperature range $M_s < T < A_f$ and above the A_f temperature. According to well-known experimental and theoretical studies, the conditions for SE are achieved at $T \geq A_f$, when martensite becomes thermodynamically unstable, when the load is removed [29,30]. SE within the temperature range from M_s to A_f was observed in FeNiCoAlNb single crystals [33], FeNiCoAlTaB [31,32] and FeNiCoTi polycrystals [9]. Reversible deformation within the temperature range between 77 K and M_s is not associated with the development of $\gamma\text{--}\alpha'$ MT under stress, but is caused by the reversible motion of “austenite-martensite” interphase and twin boundaries of a cooling α' -martensite in “load-unloading” cycles. It was previously found in FeNiCoAlNb single crystals [33] and FeNiCoAlTaB polycrystals [31,32]. This was defined as having rubber-like behavior [33]. In this paper, the reversible deformation at $T < M_s$ was not investigated.

It may be observed that σ_{cr}^{Ms} for the onset of stress-induced $\gamma\text{--}\alpha'$ MT within the temperature range from M_s to 373 K increases, with an increase in the test temperature, and the dependence, $\sigma_{cr}^{Ms}(T)$, turns out to be characteristic of alloys, undergoing MT under stress at $T > M_s$ (Figures 3 and 4). This dependence is described by the Clapeyron–Clausius relationship [29,30,45]:

$$\frac{d\sigma_{cr}^{Ms}}{dT} = -\frac{\Delta S_{ch}}{\varepsilon_{tr}} = -\frac{\Delta H_{ch}}{\varepsilon_{tr}T_0} = \alpha \quad (3)$$

ΔH_{ch} and ΔS_{ch} are the enthalpy and entropy changes, respectively, at MT; T_0 is the temperature of the chemical equilibrium of phases and ε_{tr} is the transformation strain at MT. Figure 4 demonstrates that the value $\alpha = d\sigma_{cr}^{Ms}/dT$ varies from 3.2 to 3.8 MPa/K in Crystals I–IV. In the case of Crystals II and IV, $\alpha = d\sigma_{cr}^{Ms}/dT$ is greater than for Crystals I and III. A comparison of the $\alpha = d\sigma_{cr}^{Ms}/dT$ values for Crystals I–IV with the known literature data, obtained on the [001]-oriented FeNiCoAlX crystals ($X = \text{Ta, Nb, Ti}$) under tensile strain and containing only γ' -phase particles, 3–8 nm in size and particles of the γ' - and β -phases [25,27,33,34], showed that these values, $\alpha = d\sigma_{cr}^{Ms}/dT$, are in close proximity to one other.

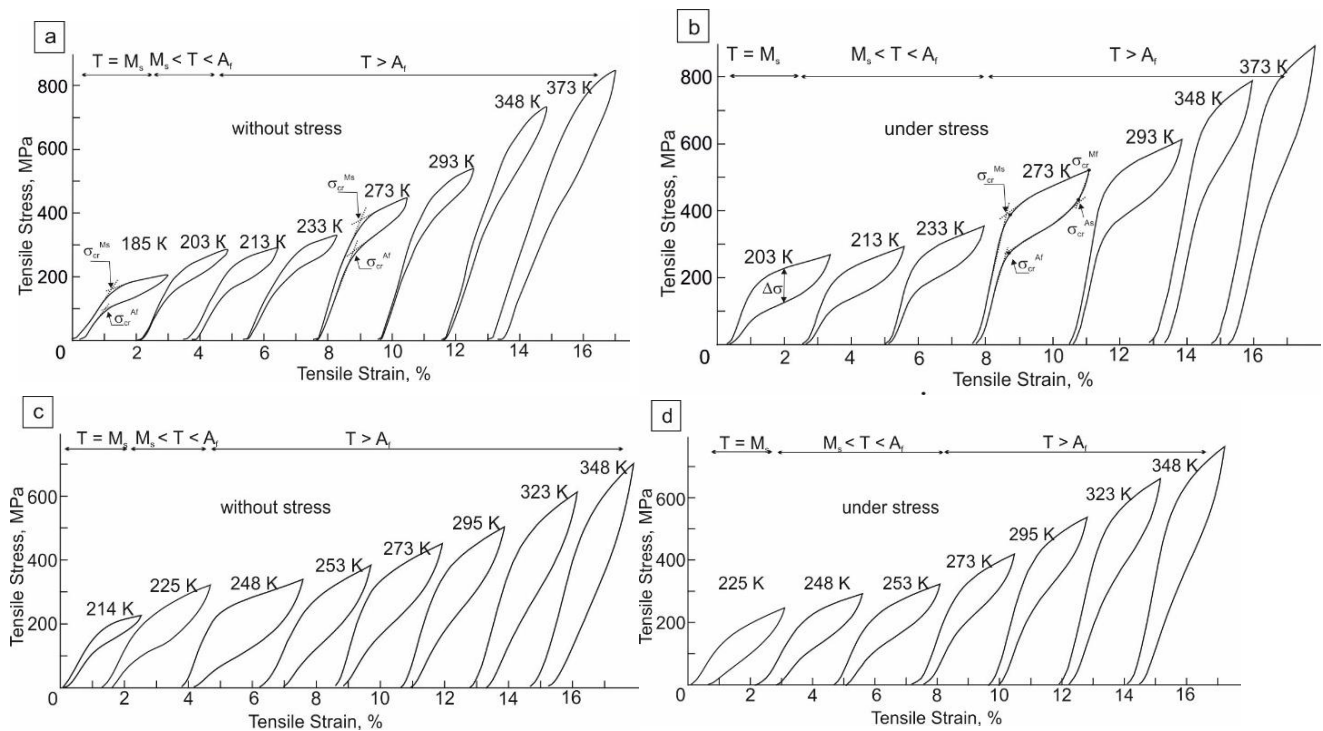


Figure 3. Temperature range of the reversible strain in the [001]-oriented FeNiCoAlNb crystals after two-step ageing under tension: (a,b)—ageing at 873 K for 2 h at the second step; (c,d)—ageing at 873 K for 4 h at the second step. Determination of critical stresses (σ_{cr}^{Ms} , σ_{cr}^{Mf} , σ_{cr}^{As} and σ_{cr}^{Af}) and value of mechanical hysteresis $\Delta\sigma$ is shown in (a,b).

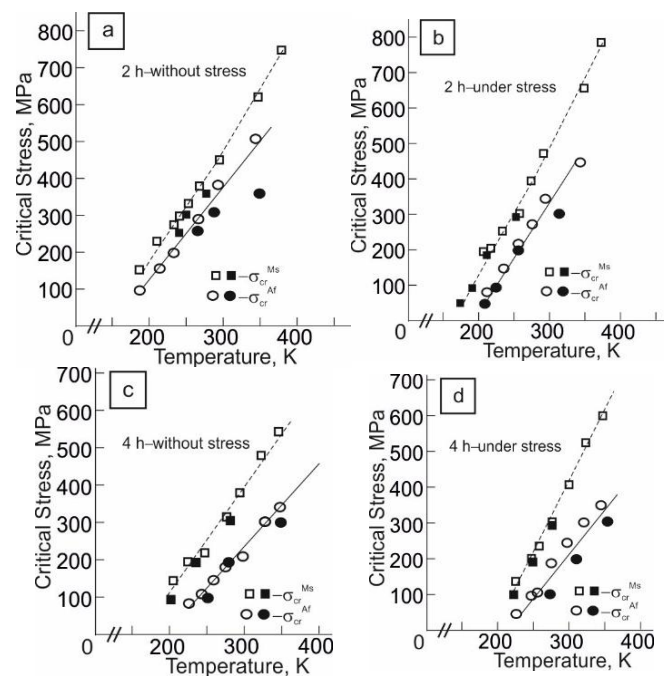


Figure 4. Temperature dependence of critical stresses, σ_{cr}^{Ms} , for the onset of stress-induced γ - α' MT and critical stresses, σ_{cr}^{Af} , for the finish reverse α' - γ MT at unloading of the [001]-oriented FeNiCoAlNb crystals after two-step ageing under tensile strain. (a,b)—ageing at 873 K for 2 h at the second step; (c,d)—ageing at 873 K for 4 h at the second step; open squares and circles are the data obtained in the study of the SE temperature range, and filled squares and circles are the data obtained in the study of the SME under stress.

Using relationship (3) and the results of an increase in the M_s temperature during ageing under stress, $\Delta M_s = M_s^\sigma - M_s^0$ (M_s^σ and M_s^0 are temperatures, respectively, in crystals aged under and without stress), one can estimate the level of internal stresses $\langle \sigma_G \rangle$ in accordance with relationship (4):

$$\langle \sigma_G \rangle = (\Delta M_s^G / \varepsilon_{tr}) \Delta S_{ch}; \Delta S_{ch} / \varepsilon_{tr} = \alpha = d\sigma_{cr} / dT \quad (4)$$

In Crystals II and IV, the value of $\langle \sigma_G \rangle$ calculated by relationship (4) is 35–57 MPa at the $\Delta M_s = 11$ –15 K and $\alpha = (3.2$ – $3.8)$ MPa/K.

SE loops with a sequential increase in ε_{tr} in the “load–unloading” cycle until fracture at M_s and the temperature above A_f of Crystals I–IV, are presented in Figure 5. The results obtained for Crystals I are close to those obtained earlier in [33]. In relation to Crystals I, at M_s temperature, the maximum SE was 3.3%. With an increase in the transformation strain, ε_{tr} , in the “load–unloading” cycle, an increase in the mechanical hysteresis, $\Delta\sigma$, is observed, and rather high values of the transformation hardening coefficient, $\Theta = d\sigma/d\varepsilon$, equal to 2 GPa, are found. At 273 K, the SE was 3%, the mechanical hysteresis, $\Delta\sigma$, increased three times relative to the M_s temperature and became equal to 170 MPa and $\Theta = 4.3$ MPa. Among Crystals II, at an M_s temperature, the SE was 3.5%, $\Delta\sigma$ increased to 135 MPa and $\Theta = d\sigma/d\varepsilon$, up to 3.2 GPa, compared to Crystals I at this temperature. At 273 K, the SE was 4%, $\Delta\sigma = 190$ MPa and $\Theta = 8$ GPa. Thus, ageing under stress leads to a significant increase in $\Theta = d\sigma/d\varepsilon$ and $\Delta\sigma$, compared to ageing without stress.

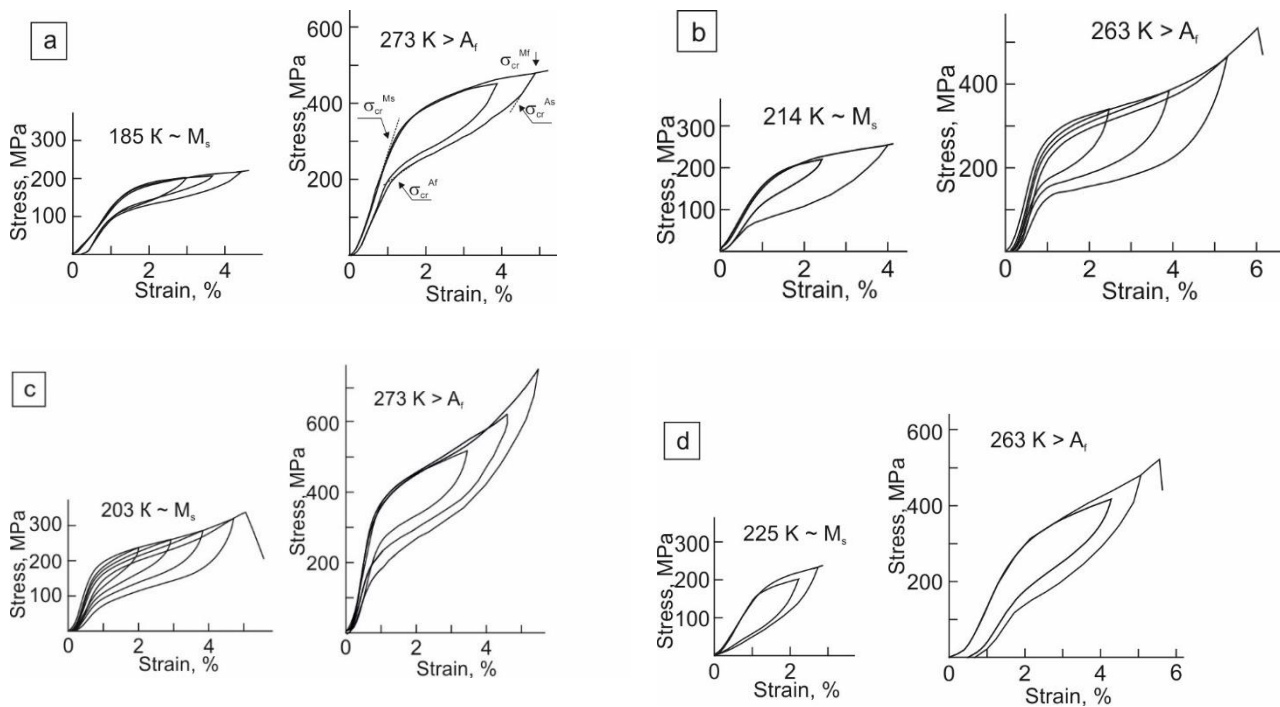


Figure 5. Tensile superelastic cycles of the [001]-oriented FeNiCoAlNb crystals after two-step ageing at different temperatures: (a)—Crystals I—ageing without stress at 873 K for 2 h at the second step; (b)—Crystals III—ageing without stress at 873 K for 4 h at the second step; (c)—Crystals II—ageing under stress at 873 K for 2 h at the second step; (d)—Crystals IV—ageing under stress at 873 K for 4 h at the second step.

In Crystals III and IV, an increase in the ageing time at the second step to 4 h at 873 K, as shown above, increases the volume fraction of β -phase particles in comparison with Crystals I and II. As a result, the SE decreases, while $\Delta\sigma$ and Θ , on the contrary, increase and an irreversible strain appears of up to 0.5% at temperatures above A_f (Figure 5).

An analysis of the SE loops for Crystals I–IV in the temperature range from M_s to 373 K, shows that in all studied crystals, the stresses, σ_{cr}^{Ms} , for the onset of stress-induced γ - α'

MT, are lower than the stresses, σ_{cr}^{As} , of the start of the reverse $\alpha'-\gamma$ MT, when unloading (Figures 3 and 5). Using the results of the thermodynamic analysis of SE loops [33,42–45], the contribution of ΔG_{el} and ΔG_{dis} can be determined from the values of σ_{cr}^{Ms} , σ_{cr}^{Mf} and σ_{cr}^{As} , σ_{cr}^{Af} :

$$\Delta G_{el} = (\sigma_{cr}^{Mf}(T) - \sigma_{cr}^{Ms}(T))\epsilon_{tr} \quad (5)$$

$$\Delta G_{dis} = \frac{1}{2}(\sigma_{cr}^{Mf}(T) - \sigma_{cr}^{As}(T))\epsilon_{tr} \quad (6)$$

σ_{cr}^{Ms} and σ_{cr}^{Mf} are the stresses at the start and end of the forward $\gamma-\alpha'$ MT under load, and σ_{cr}^{As} and σ_{cr}^{Af} are the stresses at the start and end of the reverse $\alpha'-\gamma$ MT, when the load is removed. The estimate of the ratio $\Delta G_{el}/\Delta G_{dis}$ will depend on ϵ_{tr} , therefore, its calculations for Crystals I–IV for different temperatures, were tested in relation to the close values of $\epsilon_{tr} = 2\%$ (Figure 3). Estimates showed that $\Delta G_{el}/\Delta G_{dis}$ vary from 5.5 to 6.3, within the range between M_s and A_f , and at $T > A_f$.

The condition for the appearance of a closed loop at $T \geq M_s$ was obtained in [33] according to the assumption that $\sigma_{cr}^{Af}(T) > 0$, and is written as follows:

$$\Delta G_{ch}(T) + \Delta G_{el} > \Delta G_{dis} \quad (7)$$

$\Delta G_{ch}(T) = (T - T_0)\Delta S_{ch}$ is the chemical energy change at MT. At $T \geq M_s$, condition (7) is satisfied since $\Delta G_{el} = (5.5-6.3)\Delta G_{dis}$ and the reverse $\alpha'-\gamma$ MT occurs, due to the large stored elastic energy. A high level of ΔG_{el} determines high values of the transformation hardening coefficient $\Theta = d\sigma/d\epsilon$ at $T \geq M_s$. This is due to the fact that β -phase particles have a non-coherent conjugation of the lattice with the high-temperature phase. These particles are stable and their atomic structure locks the MT inside the β -phase. Consequently, in the case of a reversible $\gamma-\alpha'$ MT, the β -phase particles are only deformed elastically and can assist to the predominant nucleation of α' -martensite near the “ β -phase–high-temperature phase” interphase surfaces, as was previously observed in the TiNi-based composites, containing TiC particles [46,47]. High values of $\Theta = d\sigma/d\epsilon$ at a low level of strain $\epsilon \leq 5\%$, were observed in fcc poly- and single crystals, containing non-coherent, plastically undeformed particles during slip deformation in Cu-SiO₂, Cu-Al₂O₃ [48,49] and upon twinning deformation in Cu-Al-Co with non-coherent CoAl particles [50]. In this case, an increase in ΔG_{el} and, accordingly, $\langle \sigma_G \rangle$, depending on the level of plastic deformation ϵ_{pl} by slip, twinning and $\gamma-\alpha'$ MT in the absence of relaxation processes, is written as [48,49]:

$$\langle \sigma_G \rangle = 2\gamma G f \epsilon_{pl} \frac{1}{m} \quad (8)$$

$$\theta \approx \frac{d\sigma_G}{d\epsilon_{pl}} = 2\gamma f G \frac{1}{m} \quad (9)$$

$\gamma = \frac{5-7\nu}{15(1-\nu)} = 0.28$, where $\nu = 0.3$ is Poisson’s coefficient for martensite, $G = 72$ GPa is the shear modulus of martensite, f is a volume fraction of β -phase particles, which is estimated as being between 10–15%, ϵ_{pl} is plastic deformation and m is the Schmid factor for twinning in the [001] orientation in martensite, which is equal to 0.41 at tensile strain [33]. The experimental $\Theta = d\sigma/d\epsilon$ values for Crystals I–IV, which ranged from 2 to 8 GPa, were close to the calculated $\Theta = d\sigma/d\epsilon$ values according to relationship (9). It is interesting that in the study of SE of the [001]-oriented FeNiCoAlX crystals ($X = Ta, Nb, Ti$), containing only the nanosized γ' -phase particles, the value of $\Theta = d\sigma/d\epsilon$ was equal to 2–3 GPa, $\sigma_{cr}^{Ms} > \sigma_{cr}^{As}$, $M_s < A_s$. Therefore, MTs are transformations of the first type, according to the Tong–Wayman classification [11,12,18,21,27].

SME studies during cooling/heating, under the constant stresses of Crystals I–IV are shown in Figures 6 and 7. The values of SME ϵ_{SME} , overcooling $\Delta M = M_s - M_f$ and overheating $\Delta A = A_f - A_s$, as well as thermal hysteresis $\Delta T_h = A_f - M_s$, depend on the level of applied stresses, σ_{cr} , in the “cooling–heating” cycle and heat treatment (Figure 6).

In the studied Crystals I–IV, the M_s^σ temperature of the onset of the γ – α' MT under stress increases with an increase in the level of applied stresses, σ_{cr} , and coincides with the M_s^σ temperature obtained in experiments on the SE study (Figures 3 and 4). The values of ΔM , ΔA , ΔT_h and ε_{tr} also increase with increasing level of applied stresses, σ_{cr} . Figure 4 displays the stresses of the finish of the reverse MT, σ_{cr}^{Af} , when the load is removed, which like the stresses for the onset of the stress-induced MT σ_{cr}^{Ms} , were obtained from the results of studying the SE temperature range (Figure 3) and the SME under stress (Figure 6). It can be seen that similar values of σ_{cr}^{Af} and σ_{cr}^{Ms} were obtained for Crystals I–IV in both experiments. The σ_{cr}^{Af} curves for Crystals I and II are parallel to the σ_{cr}^{Ms} curves, which indicates a weak dependence of $\Delta\sigma$ on the test temperature and thermal hysteresis ΔT_h on the level of external stresses. In Crystals III and IV, $\Delta\sigma$ and ΔT_h are greater than in Crystals I and II and increase with growth of the test temperature and external stresses, respectively. In this case, the σ_{cr}^{Ms} and σ_{cr}^{Af} curves are not parallel to each other. Therefore, in Crystals III and IV, $\Delta\sigma$ and ΔT_h depend, respectively, on the test temperature and external stresses. The physical reason for the stronger dependence of the $\Delta\sigma$ and ΔT_h , respectively, on the test temperature and external stresses in Crystals III and IV as compared to Crystals I and II requires additional structural studies.

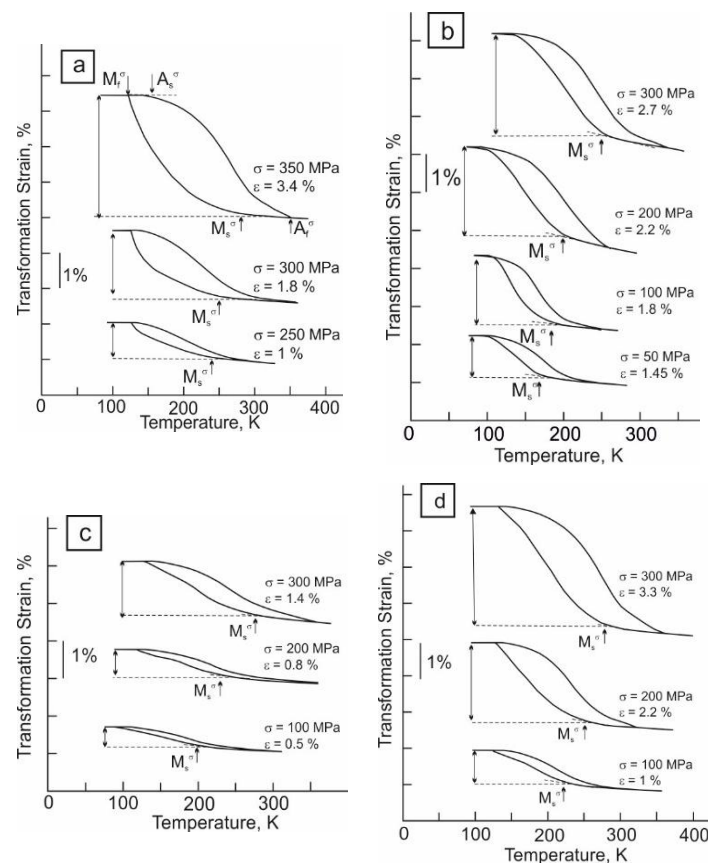


Figure 6. Strain vs. temperature response of the [001]-oriented FeNiCoAlNb crystals after two-step ageing: (a)—ageing without stress at 873 K for 2 h at the second step; (b)—ageing under stress of 120 MPa at 873 K for 2 h at the second step; (c)—ageing without stress at 873 K for 4 h at the second step; (d)—ageing under stress of 120 MPa at 873 K for 4 h at the second step.

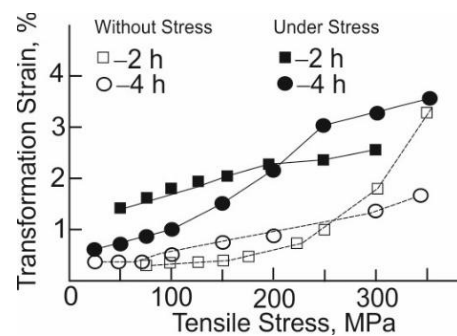


Figure 7. Transformation strain vs. tensile stress response of the [001]-oriented FeNiCoAlNb crystals after two-step ageing.

A comparison of Crystals I and III with Crystals II and IV reveals a number of differences. Firstly, the values of ε_{tr} and $d\varepsilon_{tr}/d\sigma$ in Crystals III and IV differ significantly (Figures 6 and 7). At a stress level of 300 MPa, in case of Crystals IV, ε_{tr} reaches 3.3%, whereas ε_{tr} reaches 1.4% in Crystals III. The value of ε_{tr} in these crystals is limited by their destruction. In the [001]-oriented FeNiCoAlX crystals (X = Ta, Nb, Ti), containing only the γ' -phase particles, $\varepsilon_{tr} = 5.5\text{--}8.7\%$ in experiments relating to cooling/heating under constant stress [12,18] and up to 13.5% in experiments on the SE study [5,27]. Similar results were obtained for Crystals I and II (Figures 6 and 7). Therefore, as studies of the SE and SME in single crystals containing particles of the γ' - and β -phases have shown, the particles of the β -phase lead to a decrease in the plasticity associated with the stress induced $\gamma\text{--}\alpha'$ MT.

Secondly, among Crystals I–IV at the level of constant stress of $\sigma_{cr} = 300\text{--}350$ MPa, high values of ΔM and ΔA were found, which reached 150 and 190 K; 110 and 140 K; 150 and 190 K; and 125 and 200 K, respectively, for Crystals I, II, III and IV. At the maximum level of constant stress of $\sigma_{cr} = 300\text{--}350$ MPa, the values of thermal hysteresis, ΔT_h , in Crystals I, II, III and IV are equal to 150 K, 50 K, 50 K and 100 K, respectively. In all studied crystals on the $\varepsilon_{tr}(T)$ curves under constant stress, the A_s temperature is lower than the M_s temperature (Figure 6). Therefore, such MTs under constant stress are related to the thermoelastic MT of the second type [41]. This indicates that in the [001]-oriented FeNiCoAlNb crystals, with particles of the γ' - and β -phases, a high level of ΔG_{el} accumulates at the $\gamma\text{--}\alpha'$ MT under stress. These results confirm the aforementioned conclusions regarding the second type of $\gamma\text{--}\alpha'$ MT, obtained in the study of the temperature dependence of $\rho(T)$ (Figure 1) and SE (Figures 3 and 5).

Thirdly, ageing under stress leads to the formation of internal oriented stress fields $\langle\sigma_G\rangle$, which is confirmed by an increase in the M_s temperature in Crystals II and IV as compared to Crystals I and III with the same ageing time at the second step. The source of these internal stress fields $\langle\sigma_G\rangle = 35\text{--}57$ MPa are dislocations arising at the “matrix– β -phase” interface during ageing under stress (Figure 2e). Earlier, in the [001]-oriented crystals of another Fe–28Ni–17Co–11.5Al–2.5(TiNb) (at.%) (FeNiCoAlNbTi) alloys, after ageing under stress, as in Crystals II and also containing particles of γ' - and β -phases, similar values of $\Delta M_s = 15$ K and $\langle\sigma_G\rangle = 65$ MPa were found [51].

Thus, the development of thermoelastic $\gamma\text{--}\alpha'$ MT in the [001]-oriented FeNiCoAlX crystals (X = Ta, Nb, Ti) occurs in a disordered fcc high-temperature phase, in which the nanosized γ' -phase particles with a size $d = 3\text{--}12$ nm are precipitated. The fundamental role of the γ' -phase particles is that they act as “memory elements”, which determine the restoration of the initial orientation of austenite and the realization of the fact that reverse $\alpha'\text{--}\gamma$ MT is “exactly backward” [1,2,4,5,28].

The γ' -phase particles have coherent conjugation with the high-temperature phase and retain coherence with the α' -martensite. With $d > d_{cr}$ at $\gamma\text{--}\alpha'$ MT, there is a loss of coherence of the γ' -phase with α' -martensite and relaxation of the elastic energy, ΔG_{el} , stored during the MT. As a result, the transformation becomes non-thermoelastic [1,2]. In relation to Crystals I–IV, containing particles of γ' - and β -phases, the $\gamma\text{--}\alpha'$ MT is not suppressed by the presence of the β -phase particles. In contrast to the γ' -phase particles, the β -phase particles

have non-coherent conjugation with the γ -phase and with α' -martensite. This leads to a decrease in plasticity and, accordingly, to a decrease in the value of SE and SME at MT under stress. Non-coherent β -phase particles act as preferential sites for the nucleation of α' -martensite, which grows in the regions between the β -phase. The high values of $\Theta = d\sigma/d\varepsilon$, due to MT in these crystals, which are characteristic of the development of deformation by slip and twinning [48–50], indicate an increase in ΔG_{el} with an increase in the volume fraction of α' -martensite.

The combination of a high level of ΔG_{el} and small values of ΔG_{dis} creates conditions for the development of SE within the temperature range from M_s to A_f , which are not usually observed during the development of thermoelastic MTs. Ageing under stress at the second step leads to an increase in M_s temperature, compared to ageing without stress, which is due to the appearance of the internal oriented stress fields, $\langle \sigma_G \rangle$. To elucidate the mechanism of $\langle \sigma_G \rangle$ formation, additional studies are required, in which it will be necessary to change the ageing conditions at the second step, in order to amend the size and volume fraction of the β -phase particles. This will facilitate the creation of unique composite materials, with a simultaneous precipitation of γ' - and β -phase particles, high transformation strain values and the development interval of the γ - α' MT within the high-temperature region due to a decrease in nickel in the fcc high-temperature phase, as a result of the precipitation of the β -phase particles.

In the present paper, it is shown that the maximum values of the transformation strain, ε_{tr} , obtained in experiments when studying the SE and SME during cooling/heating under constant stress, are equal to 4 and 3.4%, respectively. Theoretical estimates of ε_{tr} , carried out in [5,12], show that the value of ε_{tr} for the [001]-oriented crystals under tension decreases from 8.3 to 5.5% with an increase in the tetragonality of martensite c/a from 1.1 to 1.15%. This estimate assumes that the γ - α' MT occurs in the alloy without the γ' -phase particles or when these particles undergo elastic deformation together with the fcc matrix. The experimental values of the SME and SE under tension along the [001] direction vary from 14.5 to 5.5% for the γ' -phase particle sizes of 3 nm and 8–12 nm [5,12,18,26,27]. The non-coherent β -phase particles, the sizes of which are much larger than the γ' -phase particles, cannot accommodate transformation strain in the matrix due to elastic deformation and contribute to the generation of multiple variants of martensite from the “matrix- β -phase” interface [46,47]. As a result, ε_{tr} significantly decreases to between 3.4 and 4% and the determination of the total resource of ε_{tr} is limited by the low plasticity of Crystals I–IV due to the effect of the β -phase on transformation plasticity.

4. Conclusions

The studies of development of the thermoelastic γ - α' MT under stress using [001]-oriented FeNiCoAlNb single crystals, containing non-coherent β -phase particles after ageing under and without stress, showed that the effect of the β -phase particles on SME and SE in single crystals and polycrystals of FeNiCoAlX alloys ($X = Ta, Nb, Ti$) is fundamentally different. Based on the results of the SME and SE studies, crystal structure after ageing under and without stresses and their analysis, the following conclusions can be summarized as the main findings:

1. A new two-step ageing has been proposed for the FeNiCoAlNb single crystals, oriented along the [001]-direction for tensile strain, including ageing at the first step at 973 K for 5 h without stress and at the second step, at 873 K for 2 and 4 h without and under tensile stress at 120 MPa. At the first step of ageing at 973 K for 5 h, particles of the γ' -phase are precipitated, and at the second low-temperature step at 873 K for 2 and 4 h, a structure, consisting of particles of the γ' - and β -phases is formed.
2. An increase in the ageing time at the second low-temperature step from 2 to 4 h leads to an increase in the M_s temperature, which is associated with a decrease in the nickel concentration in the matrix due to an increase in the volume fraction of the nickel-rich β -phase particles with the composition, (FeNiCo)(AlNb).

3. Ageing under a tensile stress of 120 MPa at the second low-temperature step for 2 and 4 h leads to an increase in the M_s temperature, in comparison with ageing without stress by 11–15 K, which is associated with the generation of internal oriented tensile stresses during ageing under stress.
4. In a structure containing particles of the γ' - and β -phases, conditions are created for observing SE within the temperature range from M_s to A_f due to the formation of a high level of accumulated elastic energy, ΔG_{el} , which significantly exceeds the value of the dissipated energy, ΔG_{dis} .

Author Contributions: Conceptualization, Y.I.C. and I.V.K.; methodology, Y.I.C. and I.V.K.; investigation, I.V.K. and Z.V.P.; writing—original draft preparation, Y.I.C. and I.V.K.; writing—review and editing, Y.I.C., I.V.K., T.N. and P.K.; funding acquisition, Y.I.C. and P.K. All authors have read and agreed to the published version of the manuscript.

Funding: This research was supported by the Russian Science Foundation (project No. 19-49-04101) and by (Project No. 405372848 (KR 5134/1-1)).

Institutional Review Board Statement: Not applicable.

Informed Consent Statement: Not applicable.

Data Availability Statement: Data are available from the corresponding author on reasonable request.

Conflicts of Interest: The authors declare no conflict of interest.

References

1. Kokorin, V.V. Martensitic Transformations in Heterogeneous Solid Solutions. *Naukova Dumka* **1987**, *1987*, 165. (In Russian)
2. Hornbogen, E. The effect of variables on martensitic transformation temperatures. *Acta Met.* **1985**, *33*, 595–601. [[CrossRef](#)]
3. Hornbogen, E.; Jost, N. Alloys of iron and reversibility of martensitic transformations. *J. Phys. Colloq.* **1991**, *1*, C4-199–C4-210. [[CrossRef](#)]
4. Maki, T. Ferrous shape memory alloys. In *Book Shape Memory Material*, 1st ed.; Otsuka, K., Wayman, C.M., Eds.; Cambridge University Press: Cambridge, UK, 1998; pp. 117–132.
5. Tanaka, Y.; Himuro, Y.; Kainuma, R.; Sutou, Y.; Omori, T.; Ishida, K. Ferrous Polycrystalline Shape-Memory Alloy Showing Huge Superelasticity. *Science* **2010**, *327*, 1488–1490. [[CrossRef](#)]
6. Choi, W.S.; Pang, E.L.; Choi, P.-P.; Schuh, C.A. FeNiCoAlTaB superelastic and shape-memory wires with oligocrystalline grain structure. *Scr. Mater.* **2020**, *188*, 1–5. [[CrossRef](#)]
7. Cesari, E.; Chernenko, V.; Kokorin, V.; Pons, J.; Seguí, C. Physical properties of Fe-Co-Ni-Ti alloy in the vicinity of martensitic transformation. *Scr. Mater.* **1999**, *40*, 341–345. [[CrossRef](#)]
8. Kokorin, V.V.; Kozlova, L.E.; Titenko, A.N.; Perekos, A.E.; Levchuk, Y.S. Characteristic of thermoelastic martensitic transformation in ferromagnetic Fe-Co-Ni-Ti alloys alloyed with Cu. *Phys. Metals Metallogr.* **2008**, *105*, 564–567. [[CrossRef](#)]
9. Gunko, L.P.; Takzei, G.A.; Titenko, A.N. Thermoplastic martensitic transformation in ferromagnetic materials and their superelastic properties. *Funct. Mater.* **2002**, *9*, 75–78.
10. Geng, Y.; Lee, D.; Xu, X.; Nagasako, M.; Jin, M.; Jin, X.; Omori, T.; Kainuma, R. Coherency of ordered γ' precipitates and thermoelastic martensitic transformation in FeNiCoAlTaB alloys. *J. Alloy. Compd.* **2015**, *628*, 287–292. [[CrossRef](#)]
11. Chumlyakov, Y.I.; Kireeva, I.V.; Panchenko, E.; Kirillov, V.A.; Timofeeva, E.E.; Kretinina, I.V.; Danil'Son, Y.N.; Karaman, I.; Maier, H.J.; Cesari, E. Thermoelastic martensitic transformations in single crystals with disperse particles. *Russ. Phys. J.* **2011**, *54*, 937–950. [[CrossRef](#)]
12. Ma, J.; Hornbuckle, B.; Karaman, I.; Thompson, G.; Luo, Z.; Chumlyakov, Y. The effect of nanoprecipitates on the superelastic properties of FeNiCoAlTa shape memory alloy single crystals. *Acta Mater.* **2013**, *61*, 3445–3455. [[CrossRef](#)]
13. Czerny, M.; Maziarz, W.; Cios, G.; Wójcik, A.; Chumlyakov, Y.; Schell, N.; Fitta, M.; Chulist, R. The effect of heat treatment on the precipitation hardening in FeNiCoAlTa single crystals. *Mater. Sci. Eng. A* **2020**, *784*, 139327. [[CrossRef](#)]
14. Jin, M.; Geng, Y.; Zuo, S.; Jin, X. Precipitation and its Effects on Martensitic Transformation in Fe-Ni-Co-Ti Alloys. *Mater. Today Proc.* **2015**, *2*, S837–S840. [[CrossRef](#)]
15. Fu, H.; Li, W.; Song, S.; Jiang, Y.; Xie, J. Effects of grain orientation and precipitates on the superelasticity in directionally solidified FeNiCoAlTaB shape memory alloy. *J. Alloy. Compd.* **2016**, *684*, 556–563. [[CrossRef](#)]
16. Fu, H.; Zhao, H.; Zhang, Y.; Xie, J. Enhancement of Superelasticity in Fe-Ni-Co-Based Shape Memory Alloys by Microstructure and Texture Control. *Procedia Eng.* **2017**, *207*, 1505–1510. [[CrossRef](#)]
17. Krooß, P.; Holzweissig, M.J.; Niendorf, T.; Somsen, C.; Schaper, M.; Chumlyakov, Y.I.; Maier, H.J. Thermal cycling behavior of an aged FeNiCoAlTa single-crystal shape memory alloy. *Scr. Mater.* **2014**, *81*, 28–31. [[CrossRef](#)]

18. Ma, J.; Kockar, B.; Evirgen, A.; Karaman, I.; Luo, Z.; Chumlyakov, Y. Shape memory behavior and tension–compression asymmetry of a FeNiCoAlTa single-crystalline shape memory alloy. *Acta Mater.* **2012**, *60*, 2186–2195. [[CrossRef](#)]
19. Czerny, M.; Cios, G.; Maziarz, W.; Chumlyakov, Y.; Chulist, R. Studies on the Two-Step Aging Process of Fe-Based Shape Memory Single Crystals. *Materials* **2020**, *13*, 1724. [[CrossRef](#)] [[PubMed](#)]
20. Krooß, P.; Niendorf, T.; Karaman, I.; Chumlyakov, Y.I.; Maier, H.J. Cyclic deformation behavior of aged FeNiCoAlTa single crystals. *Funct. Mater. Lett.* **2012**, *5*, 12500454. [[CrossRef](#)]
21. Sehitoglu, H.; Karaman, I.; Zhang, X.; Chumlyakov, Y.; Maier, H.J. Deformation of FeNiCoTi shape memory single crystals. *Scr. Mater.* **2001**, *44*, 779–784. [[CrossRef](#)]
22. Chumlyakov, Y.I.; Kireeva, I.V.; Panchenko, E.Y.; Zakharova, E.G.; Kirillov, V.A.; Efimenko, S.P.; Sehitoglu, H. Shape memory effect in FeNiCoTi single crystals undergoing γ – α' thermoelastic martensitic transformations. *Doklady Phys.* **2004**, *49*, 47–50. [[CrossRef](#)]
23. Sehitoglu, H.; Efstathiou, C.; Maier, H.; Chumlyakov, Y. Hysteresis and deformation mechanisms of transforming FeNiCoTi. *Mech. Mater.* **2006**, *38*, 538–550. [[CrossRef](#)]
24. Chumlyakov, Y.; Kireeva, I.; Kuksgauzen, I.; Poklonov, V.; Pobedennaya, Z.; Bessonova, I.; Kuksgauzen, D.; Kirillov, V.; Lauhoff, C.; Niendorf, T.; et al. Shape memory effect and superelasticity in high-strength FeNiCoAlTi single crystals hardened by nanoparticles. *AIP Conf. Proc.* **2019**, *2167*, 020064. [[CrossRef](#)]
25. Chumlyakov, Y.I.; Kireeva, I.V.; Kuksgauzen, D.A.; Niendorf, T.; Krooß, P. Tension-compression asymmetry of the superelastic behavior of high-strength [001]-oriented FeNiCoAlNb crystals. *Mater. Lett.* **2021**, *289*, 129395. [[CrossRef](#)]
26. Sehitoglu, H.; Zhang, X.Y.; Kotil, T.; Canadinc, D.; Chumlyakov, Y.; Maier, H.J. Shape memory behavior of FeNiCoTi single and polycrystals. *Met. Mater. Trans. A* **2002**, *33*, 3661–3672. [[CrossRef](#)]
27. Chumlyakov, Y.; Kireeva, I.; Kutz, O.; Turabi, A.; Karaca, H.; Karaman, I. Unusual reversible twinning modes and giant superelastic strains in FeNiCoAlNb single crystals. *Scr. Mater.* **2016**, *119*, 43–46. [[CrossRef](#)]
28. Dunne, D. Martensite. *Metals* **2018**, *8*, 395. [[CrossRef](#)]
29. Otsuka, K.; Wayman, C.M. *Shape Memory Materials*; Cambridge University Press: Cambridge, UK, 1998; p. 284.
30. Otsuka, K.; Ren, X. Physical metallurgy of Ti–Ni-based shape memory alloys. *Prog. Mater. Sci.* **2005**, *50*, 511–678. [[CrossRef](#)]
31. Zhang, C.; Zhu, C.; Harrington, T.; Casalena, L.; Wang, H.; Shin, S.; Vecchio, K.S. Multifunctional Non-Equiatomic High Entropy Alloys with Superelastic, High Damping, and Excellent Cryogenic Properties. *Adv. Eng. Mater.* **2019**, *21*, 1800941. [[CrossRef](#)]
32. Zhang, C.; Zhu, C.; Shin, S.; Casalena, L.; Vecchio, K. Grain boundary precipitation of tantalum and NiAl in superelastic FeNiCoAlTaB alloy. *Mater. Sci. Eng. A* **2019**, *743*, 372–381. [[CrossRef](#)]
33. Chumlyakov, Y.; Kireeva, I.; Pobedennaya, Z.; Krooß, P.; Niendorf, T. Rubber-like behaviour and superelasticity of [001]-oriented FeNiCoAlNb single crystals containing γ' - and β -phase particles. *J. Alloy. Compd.* **2021**, *856*, 158158. [[CrossRef](#)]
34. Chumlyakov, Y.; Kireeva, I.; Kuksgauzen, I.; Poklonov, V.; Pobedennaya, Z.; Bessonova, I.; Kirillov, V.; Lauhoff, C.; Niendorf, T.; Krooß, P. Effect of β - and γ' -phase particles on the shape memory effect and superelasticity in [001]-oriented FeNiCoAlTi single crystals. *Mater. Lett.* **2020**, *260*, 126932. [[CrossRef](#)]
35. Li, D.; Chen, L. Selective variant growth of coherent Ti11Ni14 precipitate in a TiNi alloy under applied stresses. *Acta Mater.* **1997**, *45*, 471–479. [[CrossRef](#)]
36. Li, D.; Chen, L. Morphological evolution of coherent multi-variant Ti11Ni14 precipitates in Ti–Ni alloys under an applied stress—A computer simulation study. *Acta Mater.* **1998**, *46*, 639–649. [[CrossRef](#)]
37. Kireeva, I.; Picornell, C.; Pons, J.; Kretinina, I.; Chumlyakov, Y.; Cesari, E. Effect of oriented γ' precipitates on shape memory effect and superelasticity in Co–Ni–Ga single crystals. *Acta Mater.* **2014**, *68*, 127–139. [[CrossRef](#)]
38. Poster, D.A.; Easterling, K.E. *Phase Transformation in Metals and Alloys*; Chapman & Hall: London, UK, 1981; 165p.
39. Khalil-Allafi, J.; Dlouhy, A.; Eggeler, G. Ni4Ti3-precipitation during aging of NiTi shape memory alloys and its influence on martensitic phase transformations. *Acta Mater.* **2002**, *50*, 4255–4274. [[CrossRef](#)]
40. Li, J.-F.; Zheng, Z.-Q.; Li, X.-W.; Li, S.-C. Effect of compressive stress aging on transformation strain and microstructure of Ni-rich TiNi alloy. *Mater. Sci. Eng. A* **2009**, *523*, 207–213. [[CrossRef](#)]
41. Tong, H.; Wayman, C. Characteristic temperatures and other properties of thermoelastic martensites. *Acta Met.* **1974**, *22*, 887–896. [[CrossRef](#)]
42. Daróczy, L.; Palánki, Z.; Szabó, S.; Beke, D. Stress dependence of non-chemical free energy contributions in Cu–Al–Ni shape memory alloy. *Mater. Sci. Eng. A* **2004**, *378*, 274–277. [[CrossRef](#)]
43. Palánki, Z.; Daróczy, L.; Beke, D.L. Method for the Determination of Non-Chemical Free Energy Contributions as a Function of the Transformed Fraction at Different Stress Levels in Shape Memory Alloys. *Mater. Trans.* **2005**, *46*, 978–982. [[CrossRef](#)]
44. Beke, D.; Daróczy, L.; Samy, N.; Tóth, L.; Bolgár, M. On the thermodynamic analysis of martensite stabilization treatments. *Acta Mater.* **2020**, *200*, 490–501. [[CrossRef](#)]
45. Wollants, P.; Roos, J.; Delaey, L. Thermally- and stress-induced thermoelastic martensitic transformations in the reference frame of equilibrium thermodynamics. *Prog. Mater. Sci.* **1993**, *37*, 227–288. [[CrossRef](#)]
46. Vaidyanathan, R.; Bourke, M.; Dunand, D. Phase fraction, texture and strain evolution in superelastic NiTi and NiTi–TiC composites investigated by neutron diffraction. *Acta Mater.* **1999**, *47*, 3353–3366. [[CrossRef](#)]
47. Dunand, D.C.; Mari, D.; Bourke, M.A.M.; Roberts, J.A. NiTi and NiTi–TiC composites: Part IV. Neutron diffraction study of twinning and shape-memory recovery. *Met. Mater. Trans. A* **1996**, *27*, 2820–2836. [[CrossRef](#)]

48. Martin, J.W. *Micromechanisms in Partical-Hardened Alloys*; Cambridge Solid State Science Series; Cambridge University Press: Cambridge, UK, 1980; p. 197.
49. Brown, L. Back-stresses, image stresses, and work-hardening. *Acta Met.* **1973**, *21*, 879–885. [[CrossRef](#)]
50. Korotaev, A.D.; Chumlyakov, Y.I.; Esipenko, V.F.; Bushnev, L.S. Superelasticity effects in single crystals of Cu-15% Al-2% Co with non-coherent particles due to twinning. *Phys. Status Solidi A* **1984**, *82*, 405–412. [[CrossRef](#)]
51. Chumlyakov, Y.; Kireeva, I.; Pobedennaya, Z.; Kuksgauzen, I.; Poklonov, V.; Krooß, P.; Niendorf, T.; Lauhoff, C.; Vollmer, M. Shape memory effect and superelasticity in high-strength FeNiCoAlTiNb single crystals. *AIP Conf. Proc.* **2020**, *2310*, 020065. [[CrossRef](#)]